Diffusion Coefficients of *n*-Butylbenzene, *n*-Pentylbenzene, 1-Phenylhexane, 1-Phenyloctane, and 1-Phenyldodecane in Supercritical Carbon Dioxide.

Consuelo Pizarro, Octavio Suárez-Iglesias, Ignacio Medina*, and Julio L. Bueno

Departamento de Ingeniería Química y T.M.A., Universidad de Oviedo

33071 Oviedo, Spain

e-mail: medina@uniovi.es

Abstract

Binary diffusion coefficients at infinite dilution in supercritical carbon dioxide, D_{AB}, were measured for five *n*-alkylbenzenes (*n*-butylbenzene, *n*-pentylbenzene, 1-phenylhexane, 1-phenyloctane and 1-phenyldodecane) by means of the Taylor-Aris technique in a chromatographic apparatus from 313 to 333 K and from 15.0 to 35.0 MPa. The experimental results were correlated with temperature, pressure, solvent viscosity and solvent density. In the case of temperature dependence, additional measurements were carried out for *n*-pentylbenzene from 308 to 398 K at 35.0 MPa. As the five solutes are similar molecules, the corresponding states principle of Teja was tested together with the results obtained from several predictive equations based on the Stokes-Einstein formula and on the rough-hard-sphere model.

Keywords: Diffusion; Carbon Dioxide; Chromatography; Corresponding States Principle; n-Alkylbenzenes

---

1. Introduction

In recent years a tremendous amount of attention has been paid to the area of supercritical fluids. Supercritical fluid solvents are now used for a large variety of applications. The reason is that these fluids have several superior inherent properties, including a higher diffusivity and a lower viscosity than that of a liquid, and a stronger solvent power than a gas. Moreover, the solutes dissolved in the supercritical fluid can be recovered when the fluid expands.

Supercritical carbon dioxide has been widely used in industrial, environmental, pharmaceuttical, and fundamental studies. Carbon dioxide is one of the most commonly used supercritical fluids because it is an easy gas to handle; it is inert, nontoxic and non flammable; and it has a convenient critical temperature. On the other hand, its limitations are a lack of polarity and capacity to form specific solvent-solute interactions. To improve its polarity, the addition of a small amount of suitable cosolvent can greatly enhance its solvent power.

Information on solubilities and transport properties such as diffusivity, viscosity, and thermal conductiviy in supercritical carbon dioxide is of vital importance in order to efficiently design extraction procedures. The diffusion coefficient of solutes in supercritical carbon dioxide is one of the most useful transport properties which must be fully understood and correctly modelled for the process of supercritical carbon dioxide extraction to be developed successfully. In the last three decades, the diffusion coefficient of a large number of compounds in supercritical carbon dioxide has been measured, reported, and reviewed.[1-3] However, literature data on these systems are scarce and the development of new processes and new applications has maintained the need for new experimental diffusion determinations.

Measuring the solute diffusion coefficient in supercritical carbon dioxide can be accomplished by various methods: by the solid dissolution technique, by means of photon correlation spectroscopy or light scattering, by the nuclear magnetic resonance technique, by the Stefan tube, or Taylor-Aris dispersion techniques.[4] The most widely used method for determining diffusion coefficients is the Taylor-Aris peak broadening technique. The principle on which this technique is based is that the dispersion of a pulse of a test substance in a fully developed laminar flow is due to the combined action of convection parallel to the axis and the molecular diffusion in the radial direction. The diffusion coefficient can be obtained from an analysis of the peak shape.

In this work, the diffusion coefficients of *n*-butylbenzene, *n*-pentylbenzene, 1-phenylhexane, 1-phenyloctane and 1-phenyldodecane were measured in supercritical carbon

dioxide at 313, 323 and 333 K over the pressure range of 15.0 to 35.0 MPa by the Taylor-Aris dispersion method. The data were correlated with temperature, pressure, solvent density and solvent viscosity. The values of the diffusion coefficients measured were compared with the values calculated by numerous predictive equations. These equations are based on modifications of the Stokes-Einstein equation and on the Enskog kinetic theory of hard sphere fluids. As the five solutes are similar molecules, the corresponding states principle (CSP) was applied as well.

In a previous work,[5] the authors have extended two published corresponding states models to the supercritical region. In supercritical fluids, such as carbon dioxide, the CSP has not been analyzed in a rigorous way. The five solutes are simple aromatic molecules and can be employed to evaluate the ability of CSP to calculate the diffusion coefficients of one compound from these of homologous molecules. The five solutes do not form intramolecular hydrogen bonds and cannot interact with the carbon dioxide.

2. Theoretical Background

2.1. The Taylor-Aris Technique. The diffusion coefficients were measured using the Taylor-Aris technique. When a pulse of solute is injected into a pure solvent flowing in a slow laminar flow, this pulse will disperse due to the combined effects of molecular diffusion and axial bulk flow. The pulse of a solute, after a sufficient residence time, becomes normally distributed, and the diffusion coefficient can be obtained from an analysis of the peak shape.

The binary diffusion coefficient of the solute in the supercritical fluid, D_{AB}, can be obtained by means of the following expression:

$$D_{AB} = \frac{U_0}{4}\left[H \pm \sqrt{H^2 - \frac{r_0^2}{3}}\right] \tag{1}$$

where H is the height of the theoretical plate, U_0 is the average velocity of the mobile phase and r_0 is the inner radius of the dispersion tube. The theoretical plate height is experimentally determined by first measuring the width of the peak at 0.607 times the peak height.

Detailed reviews of the criteria for the design and operation of the Taylor dispersion method are given by Liong et al.,[6] Levelt-Sengers et al.,[7] Bueno et al.[8] and Gonzalez et al.[9]

2.2. Predictive Equations. Binary diffusion at low densities is easily estimated by the theoretically developed Chapman-Enskog formula.[10] Nevertheless, in compressed gases and liquids, molecular simulations or semiempirical equations must be employed due to the lack of reliable theories. Computer simulations of molecular movements can help to understand experimental results and can provide microscopic information that is absent in the semiempirical models.[11–21] However, they are time-consuming and, if D_{AB} is measured at finite concentrations, bad statistical evaluations are produced. Semiempirical formulas are more useful from an engineering point of view, although it is difficult to known "a priori" which one of the many available will provide the best predictions. These equations can be roughly classified into two groups: the Stokes-Einstein type and the rough-hard-sphere type. To the first class belong Scheibel,[22] Wilke-Chang,[22] Reddy-Doraiswamy,[23] Lusis-Ratcliff,[24] King-Hsue-Mao,[25] Sitaraman-Ibrahim-Kuloor,[26] Tyn-Calus,[27] Umesi-Danner,[28] Lai-Tan,[29] Kooijman,[30] Liu-Ruckenstein[31] and Woerlee.[32] The second class includes formulas related to Dymond free-volume and molecular simulations, e. g. those of Catchpole-King,[33] Eaton-Akgerman,[34] He of 1997,[35] He of 1998,[36] He-Yu of 1997,[37] He-Yu of 1998,[38] Liu-Silva-Macedo,[39] Funazukuri-Hachisu-Wakao,[40] Funazukuri-Kong-Kagei,[41-43] Dariva-Coelho-Oliveira[19,44,45], Zhu-Lu-Zhou-Wang-Shi[46] and Rah-Kwak-Eu-Lafleur.[47]

2.3. The Corresponding States Principle. The CSP was proposed by van der Waals in 1873 to estimate the compressibilities of pure fluids,[22] and Teja extended it to self-diffusivities and binary diffusivities in 1985.[48] At the same temperature and pressure of solvent B, the unknown diffusivity of solute A, D_{AB}, can be calculated from the diffusivities of the other two solutes 1 and 2 in the same solvent (molecules 1 and 2 being similar to A) as follows:

$$\left(\frac{D_{AB}M_A^{1/2}}{T_{cA}^{1/2}V_{cA}^{1/3}}\right)=\left(\frac{D_{1B}M_1^{1/2}}{T_{c1}^{1/2}V_{c1}^{1/3}}\right)+\frac{\theta_A-\theta_1}{\theta_2-\theta_1}\left[\left(\frac{D_{2B}M_2^{1/2}}{T_{c2}^{1/2}V_{c2}^{1/3}}\right)-\left(\frac{D_{1B}M_1^{1/2}}{T_{c1}^{1/2}V_{c1}^{1/3}}\right)\right] \qquad (2)$$

where T_c and V_c are the critical temperature and volume respectively, and M the molecular mass. The parameter θ can be taken as $V_c^{2/3}$ or equal to the acentric factor, ω.

3. Experimental Section

A flow-type apparatus was used to measure the diffusion coefficients of *n*-butylbenzene, *n*-pentylbenzene, 1-phenylhexane, 1-phenyloctane and 1-phenyldodecane in supercritical carbon dioxide. A Hewlett-Packard G1205A supercritical fluid chromatograph (SFC) was employed throughout this work. The HP SFC system consists of a pumping module, a column oven, a manual injection valve, a multiple wavelength UV detector (MWD), a modifier pump, a mass flow sensor, a HP Vectra PC and a HP printer. [49, 50]

The oven module is able to accommodate capillary and standard HPLC columns. The HP SFC uses both gas and liquid-phase detectors. In the present work, this unit uses a multiple wavelength UV detector (MWD). The HP SFC uses an electrothermally cooled reciprocating pump to supply supercritical fluids to the system. Electrothermal cooling ensures a clean, self-contained, quiet, and reliable operation. The pump has feedback control, which compensates for fluid compressibility, minimizes pressure ripple, and provides more reproducible results. In addition, the use of a reciprocating pump eliminates the inconvenience associated with refilling syringe pumps. The variable restrictor is a programmable, backpressure control device located inside the pump module. The variable restrictor consists of a pressure transducer and a nozzle, which opens and closes accordingly, releasing mobile phase in order to control pressure. Flow rate and column outlet pressure are independently controlled by the system. The SFC ChemStation consists of a PC and HP SFC software. The SFC ChemStation allows instrument control and data handling on a Microsoft Windows-based platform. The mass flow sensor is located inside the pumping module.

The solutes used during this study n-butylbenzene, n-pentylbenzene, 1-phenylhexane, 1-phenyloctane and 1-phenyldodecane were obtained from Merck (synthesis grade). The *n*-butylbenzene, *n*-pentylbenzene, and 1-phenyloctane had a minimum purity of 98% and the 1-phenylhexane, and the 1-phenyldodecane a minimum purity of 97%. The chemicals were used without further purification. The carbon dioxide supplied by Air Liquide had a minimum purity of 99.998%.

The wavelengths of the light source were set to 255, 261, and 268 nm for the *n*-butylbenzene; 259, 261, and 263 nm for the *n*-pentylbenzene; 265, 268, and 270 nm for the 1-phenylhexane; 259, 261, and 263 nm for the 1-phenyloctane, and 259, 260, and 261 nm for the 1-phenyldodecane.

The diffusion column consisted of one stainless steel tube (0.762 mm i.d. and 30.48 m in length). The uncertainty for the oven temperature and column pressure was 1 K and 0.1

MPa, respectively. The experiments were carried out over long periods of time. Typically, a flow rate of 0.12-0.14 g/min was used over a period of 10-12 h. The solutes were injected at intervals of 12-15 min, to prevent any overlapping of the solute peaks. Seven to ten injections were performed for each diffusion coefficient data point. The percentage relative standard deviations were found to be within 2%, reflecting the reasonable accuracy of the experimental data.

4. Experimental Results and Discussion

The experimental results for the five alkylbenzenes are compiled in Table 1, together with the density[51] and viscosity[52] of the solvent. Diffusivities range from 13.87×10^{-9} to 4.73×10^{-9} m^2/s and as was expected, when the mass and size of the molecule increase, the diffusion coefficient disminishes. Figure 1 shows the dependence of D_{AB} on the number of carbon atoms in the radical chain at several experimental conditions. Benzene, toluene, ethylbenzene and *n*-propylbenzene points were also included.[53]

Figure 2 illustrates the pressure dependence of *n*-butylbenzene. As the influence of pressure at elevated pressures is lower than at low pressures, Suarez et al.[53] proposed the following correlation at isothermical conditions:

$$D_{AB} = a_P + b_P / P \tag{3}$$

When the temperature increases, the pressure effect on the diffusion coefficients also increases, because the parameter b_P rises with T.

Figure 3 shows the temperature dependence of *n*-pentylbenzene. At constant pressure, diffusivities can be correlated in the form of an Arrhenius-type equation.[53,54] b_T tends to be lower at high pressures, so the molecular movements are less hindered at low pressures.

$$ln\left(\frac{D_{AB}.10^9}{m^2/s}\right) = a_T + \frac{b_T}{T} \tag{4}$$

Table 2 also contains some additional data in $1.01 \leq T_{rB} \leq 1.31$ range that we obtained for *n*-pentylbenzene at 35.0 MPa with the aim of carrying out a more thorough study of

temperature dependence. Other researchers have proposed logarithmic [55] and linear [56, 57] correlations in the form of eqs 5 and 6, respectively, but the regression coefficient for the Arrhenius-type expression is the best. Figure 4 shows the results of fitting the parameters of this table to eq 4. In the last case, the maximum deviation is only 4.88% for 398 K, a temperature 65 K higher than the limit of applicability for the aforesaid parameters.

$$ln\left(\frac{D_{AB}.10^9}{m^2/s}\right) = a_T^{(I)} + b_T^{(I)}\, ln\left(\frac{T}{K}\right) \tag{5}$$

$$D_{AB} = a_T^{(II)} + b_T^{(II)} T \tag{6}$$

Concerning the isothermical variation of the diffusivities with solvent density, a linear relationship can be established in the form [57, 58]

$$D_{AB} = a_\rho + b_\rho \rho_B \tag{7}$$

Figure 5 illustrates this linear tendency for *n*-hexylbenzene. Nevertheless, this density dependence is similar to that proposed by Grushka et al.[59] for diffusion in liquids

$$D_{AB}/T = a_{\rho T} + b_{\rho T}\, \rho_B \tag{8}$$

The regression coefficients are good and are only slightly lower than the average of the individual values of *R* for eq 7.

The effect of viscosity on diffusivities is shown, by way of example, for 1-phenyloctane in Figure 6. When η_B increases at constant temperature, D_{AB} decreases, in agreement with the the Stokes-Einstein model [53, 60-62]

$$D_{AB} = a_\eta + b_\eta/\eta_B \quad \text{at each temperature} \tag{9}$$

$$D_{AB}/T = a_{\eta T} + b_{\eta T}/\eta_B \quad \text{at any condition} \tag{10}$$

Despite the good correlations, according to the original model, the parameters a_T and a should be zero, which indicates some degree of failure in the Stokes-Einstein's postulates.

5. Predicting Diffusion Data

As previously mentioned, the Stokes-Einstein formula and the rough-hard-sphere theory provide the basis for semiempirical approaches. In the first case, the binary diffusion coefficient at infinite dilution is described as[63]

$$D_{AB} = \frac{kT}{3\pi\sigma_A\eta_B} \tag{11}$$

where k is the Boltzmann constant and σ_A the molecular diameter of the solute.

The rough-hard-sphere theory is developed from the Enskog-Thorne model for hard-spheres.[10] Computer molecular simulations[64, 65] correct the shortcoming of the model through a function F_D and attractive forces are introduced through a rotational-translational coupling parameter, C_D and effective diameters (which are temperature dependent).[66]

$$D_{AB} = \frac{3C_D}{8n_B(\sigma_{AB}^{eff})^2}\sqrt{\frac{kT}{\pi m_{AB}}}\frac{F_D}{g(\sigma_{AB}^{eff})} \tag{12}$$

n_B is the number density of solvent, g(σ_{AB}), the radial distribution function for hard spheres, σ_{AB} , the solute-solvent mean diameter and m_{AB}, the molecular mean mass of the system. Among these models, the well-known free volume theory of Dymond[67] establishes that the group $D_{AB}/T^{1/2}$ is a linear function of the molar volume of the solvent.

The properties necessary for the calculations were compiled in Table 3. The first six are from the KDB, the radius of gyration from HYSYS software and the latent heats of vaporization have been taken from the CRC Press handbook.[68] Van der Waals size parameters were calculated with ChemDraw 3D software, the parachors by a group contribution method, [22] and the volumes at boiling point by means of the Tyn and Calus equation,[22] except for carbon dioxide, whose value was known.[69] The Average Absolute Deviation (AAD) of the Stokes-Einstein type and rough-hard-sphere type expressions are given in Table 4 together with the errors of eq 2, benzene being selected as fluid 1 (to improve the predictive ability of the Teja model) and 1-phenyldodecane or 1-octylbenzene as fluid 2.

The Liu-Ruckenstein model [31] also needs the binary interaction constants of the Peng-Robinson equation of state. They are k_{ij}=0.120 for butylbenzene, k_{ij}=0.111 for pentylbenzene, both taken from Gironi and Lavechia[70] , and k_{ij} =0.101 for the others because this is the value recommended by HYSYS and it is very near to the value of 0.1 obtained for the equation of state of Soave.[71] The interaction constants of both equations of state are similar.

The self-diffusivities of carbon dioxide required for the Rah-Kwak-Eu-Lafleur formula were interpolated from Groβ et al.[72]

It must be pointed out that the equations of Wilke-Chang, Woerlee, Liu-Silva-Macedo and Dariva-Coelho-Oliveira tend to subestimate D_{AB}, whereas the expressions of Scheibel, Reddy-Doraiswamy, Lusis-Ratcliff, King-Hsue-Mao, Lai-Tan, Kooijman, Liu-Ruckenstein and He of 1998 tend to overestimate the diffusivities. The values predicted by Tyn-Calus and Sitaraman-Ibrahim-Kuloor are lower than the experimental ones for all the solutes except for dodecylbenzene, which are higher. Thus, as most of the predictive equations show the AAD for dodecylbenzene differs considerably from those of the other alkylbenzenes. The best represented solute is n-butylbenzene because no fewer than fourteen formulas show that it has the least AAD.

Errors lower than 10% for the five solutes are only obtained with the formulas of Wilke-Chang, Catchpole-King and Rah-Kwak-Eu-Lafleur. The results of the CSP of Teja are also very good if θ is taken as $V_c^{2/3}$. The worst predictions are given by the Stokes-Einstein type expressions: Reddy-Doraiswamy, Lai-Tan, Kooijman and Woerlee.

When fluid 1=benzene and fluid 2=octylbenzene, eq 2 with $\theta = V_c^{2/3}$ gives deviations lower than 6% for the other four solutes and is therefore the best of all the predictive equations compiled in Table 5. Bearing in mind that the acentric factor is a measurement of non-sphericity and that $V_c^{2/3}$ is related with the surface area of the diffusing species, a comparison of the calculated results with the experimental data clearly shows that area is the determining property in binary diffusion at infinite dilution, together with molar mass, critical temperature and critical volume.

The equations in Table 5 with an AAD<10% for *n*-pentylbenzene were selected to predict the diffusivities of this solute at 35.0 MPa and $306 \leq T \leq 398$ K versus the experimental ones. The deviations are compiled in Table 5. Liu-Ruckenstein and Eaton-Akgerman are limited to T_r<1.1, and Catchpole-King to T_r<1.25, so neither of them can be employed in the full range of temperatures. Figure 7 reveals the huge overestimation of Scheibel and He of 1998 at high

temperatures, and the underestimation achieved by the two formulas of Funazukuri et al. The best estimations were obtained with the model of He of 1997.

6. Conclusions

This paper presents data relating to the binary diffusivities of *n*-butylbenzene, *n*-pentylbenzene, 1-phenylhexane, 1-phenyloctane and 1-phenyldodecane in carbon dioxide under supercritical conditions. As was expected, heavier and larger alkylbenzenes diffuse more slowly than lighter and smaller ones. An increase in pressure, density or viscosity at constant temperature causes a decrease in diffusion. If the temperature rises and the other three variables remain unchanged, diffusivity increases.

Several predictive equations were tested against the experimental data. The best of all was the Teja formula (1985), inspired by the Corresponding States Principle.

Acknowledgement

The authors are grateful to the Ministry of Education and Science of Spain, for financially supporting this research work through project PPQ2001-3619.

Supporting Information Available

Fitting parameters and regression coefficients of equations 3-10.

Symbols

AAD	average absolute deviation
A^{vdW}	van der Waals area, m^2/molecule
a_P	fitting constant of eq 3, m^2/s
a_T	fitting constant of eq 4
$a_T^{(I)}$	fitting constant of eq 5
$a_T^{(II)}$	fitting constant of eq 6, m^2/s

a_η	fitting constant of eq 9, m^2/s
$a_{\eta T}$	fitting constant of eq 10, $m^2/K\ s$
a_ρ	fitting constant of eq 7, m^2/s
$a_{\rho T}$	fitting constant of eq 8, $m^2/K\ s$
b_P	fitting constant of eq 3, $MPa\ m^2/s$
b_T	fitting constant of eq 4, K^{-1}
$b_T^{(I)}$	fitting constant of eq 5
$b_T^{(II)}$	fitting constant of eq 6, $m^2/K\ s$
B_η	fitting constant of eq 9, kg m/s
$b_{\eta T}$	fitting constant of eq 10, kg m/K s
B_ρ	fitting constant of eq 7, $m^5/s\ kg$
$b_{\rho T}$	fitting constant of eq 8, $m^5/K\ s\ kg$
C_D	rotational-translational coupling parameter
D_{AB}	binary diffusivity at infinite dilution, m^2/s
F_D	corrective function
$g(\sigma_{AB})$	radial distribution function
H	height of the theoretical plate, m
K	Boltzmann constant
M	molar mass, kg/mol
M	molecular mass, kg/molecule
N	number density, $molecules/m^3$
P	pressure, Pa
R	regression coefficient
r_0	dispersion tube inner radius, m
r_g	radius of gyration, m
T	absolute temperature, K
U_0	mean velocity of the solvent, m/s
V	molar volume, m^3/mol
V^{vdw}	van der Waals volume, m^3/molecule
ΔH_v	heat of vaporization, J/mol

Greek symbols

θ	parameter of eq 2
η	viscosity, kg/m s
ρ	density, kg/m^3
σ	molecular diameter, m
ω	acentric factor

Subscript

A	solute
B	solvent
b	boiling point
c	critical point

Superscript

eff	effective

Literature cited

1. Suárez, J. J.; Medina, I.; Bueno, J. L. Diffusion Coefficients in Supercritical Fluids: Available Data and Graphical Correlations. *Fluid Phase Equilib.* **1998**, *153*, 167.

2. Higashi, H.; Iwai, Y.; Arai, Y. Solubilities and Diffusion Coefficients of High Boiling Compounds in Supercritical Carbon Dioxide. *Chem. Eng. Sci.* **2001**, *56*, 3027.

3. Funazukuri, T.; Kong, C. Y.; Kagei, S. Binary Diffusion Coefficients in Supercritical Fluids: Recent Progress in Measurements and Correlations for Binary Diffusion Coefficients. *J. Supercrit. Fluids* **2006**, *38*, 201.

4. Ozguler, E. I.; Sunol, S. G.; Sunol, A. K. Analysis of the Stefan Tube at Supercritical Conditions and Diffusion Coefficient Measurements. *Ind. Eng. Chem. Res*. **2003**, *42*, 4389.

5. González, L. M.; Suárez-Iglesias, O.; Bueno, J. L.; Pizarro, C.; Medina, I. Application of the Corresponding States Principle to the Diffusion in CO_2. *AIChE J*. **2007**, *53*, 3054.

6. Liong, K. K.; Wells, P. A.; Foster, N. R. Diffusion in Supercritical Fluids. *J. Supercrit. Fluids* **1991**, *4*, 91.

7. Levelt Sengers, J. M. H.; Deiters, U. K.; Klask, U.; Swidersky, P.; Schneider, G.M. Application of the Taylor Dispersion Method in Supercritical Fluids. *Int. J. Thermophys.* **1993**, *14*, 893.

8. Bueno, J. L.; Suárez, J. J.; Dizy, J.; Medina, I. Infinite Dilution Diffusion Coefficients: Benzene Derivatives as Solutes in Supercritical Carbon Dioxide. *J. Chem. Eng. Data* **1993**, *38*, 344.

9. González, L. M.; Bueno, J. L.; Medina, I. Measurement of Diffusion Coefficients for 2-Nitroanisole, 1,2-Dichlorobenzene and tert-Butylbenzene in Carbon Dioxide Containing Modifiers. *J. Supercritic. Fluids* **2002**, *24*, 219.

10. Hirschfelder, J. O.; Curtiss, C. F.; Bird, R. B. *Molecular Theory of Gases and Liquids*; John Wiley & Sons: New York, 1964.

11. Jacucci, G.; McDonald, I. R. Structure and Diffusion in Mixtures of Rare-Gas Liquids. *Physica A*. **1975**, *80*, 607.

12. Stoker, J. M.; Rowley, R. L. Molecular Dynamics Simulation of Real-Fluid Mutual Diffusion Coefficients with the Lennard-Jones Potential Model. *J. Chem. Phys*. **1989**, *91*, 3670.

13. Rowley, R. L.; Stoker, J. M.; Gile, N. F. Molecular Dynamics Simulation of Mutual Diffusion in Nonideal Liquid Mixtures. *Int. J. Thermophys*. **1991**, *12*, 501.

14. Zhou, Y.; Miller, G. H. Mutual Diffusion in Binary Ar-Kr Mixtures and Empirical Diffusion Models. *Phys. Rev. E*. **1996**. *53*, 1587.

15. Keffer, D. J.; Adhangale, P. The Composition Dependence of Self and Transport Diffusivities from Molecular Dynamics Simulations. *Chem. Eng. J*. **2004**, *100*, 51.

16. Zhou, Z.; Todda, B. D.; Travis, K. P., Sadus, R. J. A Molecular Dynamics Study of Nitric Oxide in Water: Diffusion and Structure. *J. Chem. Phys*. **2005**, *123*, 054505/1.

17. Higashi, H.; Iwai, I.; Uchida, H.; Arai, Y. Diffusion Coefficients of Aromatic Compounds in Supercritical Carbon Dioxide Using Molecular Dynamics Simulation. *J. Supercrit. Fluids* **1998**, *13*, 93.

18. Higashi, H.; Iwai, I.; Arai, Y. Calculation of Self-Diffusion and Tracer Diffusion Coefficients Near the Critical Point of Carbon Dioxide Using Molecular Dynamics Simulation. *Ind. Eng. Chem. Res*. **2000**, *39*, 4567.

19. Coelho, L. A. F.; Marchut, A.; De Oliveira, J. V.; Balbuena, P. B. Theorectical Studies of Energetics and Diffusion of Aromatic Compounds in Supercritical Carbon Dioxide. *Ind. Eng. Chem. Res*. **2000**, *39*, 227.

20. Zhou, J.; Lu, X.; Wang, Y.; Shi, J. Molecular Dynamics Investigation on the Infinite Dilute Diffusion Coefficients of Organic Compounds in Supercritical Carbon Dioxide. *Fluid Phase Equilib*. **2000**, *172*, 279.

21. Higashi, H.; Iwai, I.; Arai, Y. Comparison of Molecular Models Used in Molecular Dynamics Simulation for Tracer Diffusion Coefficients of Naphthalene and Dimethylnaphthalene Isomers in Supercritical Carbon Dioxide. *Fluid Phase Equilib*. **2005**, *234*, 51.

22. Reid, R.C.; Prausnitz, J.M.; Poling, B.E. *The Properties of Gases and Liquids* (4^{th} ed); McGraw-Hill. Inc: New York, **1987**.

23. Reddy, K. A.; Doraiswamy, L. K. Estimating Liquid Diffusivity. *Ind. Eng. Chem. Fundam.* **1967**, *6*, 77.

24. Lusis, M. A.; Ratcliff, G. A. Diffusion in Binary Liquid Mixtures at Infinite Dilution. *Can. J. Chem. Eng.* **1968**, *46*, 385.

25. King, C. J.; Hsueh, L.; Mao, K. W. Liquid-Phase Diffusion of None Electrolytes at High Dilution. *J. Chem. Eng. Data.* **1965**, *10*, 348.

26. Sitaraman, R.; Ibrahim, S. H.; Kuloor, N. R. Generalized Equation for Diffusion in Liquids. *J. Chem. Eng. Data.* **1963**, *8*, 198.

27. Tyn, M. T.; Calus, W. F. Diffusion Coefficients in Dilute Binary Liquid Systems. *J. Chem. Eng. Data.* **1975**, *20*, 106.

28. Umesi, N. O.; Danner, R. P. Predicting Diffusion Coefficients in Nonpolar Solvents. *Ind. Eng. Chem. Proc. Design Develop.* **1981**, *20*, 662.

29. Lai, C.-C.; Tan, C.-S. Measurement of Molecular Diffusion Coefficients in Supercritical Carbon Dioxide Using a Coated Capillary Column. *Ind. Eng. Chem. Res*. **1995**, *34*, 674.

30. Kooijman, H. A. A Modification of the Stokes-Einstein Equation for Diffusivities in Dilute Binary Mixtures. *Ind. Eng. Chem. Res.* **2002,** *41*, 3326.

31. Liu, H.; Ruckenstein, E. Predicting the Diffusion Coefficients in Supercritical Fluids. *Ind. Eng. Chem. Res*. **1997**, *36*, 888. Correction in *Ind. Eng. Chem. Res*. **1998**, *37*, 3524.

32. Woerlee, G. F. Expression for the Viscosity and Diffusivity Product Applicable for Supercritical Fluids. *Ind. Eng. Chem. Res*. **2001**, *40*, 465.

33. Catchpole, O. J.; King, M. B. Measurement and Correlation of Binary Diffusion Coefficients in Near Critical Fluids. *Ind. Eng. Chem. Res*. **1994**, *33*, 1828. Correction in *Ind. Eng. Chem. Res*. **1997**, *36*, 4013.

34. Eaton, A. P.; Akgerman, A. Infinite-Dilution Diffusion Coefficients in Supercritical Fluids. *Ind. Eng. Chem. Res*. **1997**, *36*, 923.

35. He, C.-H. Prediction of Binary Diffusion Coefficients of Solutes in Supercritical Solvents. *AIChE J.* **1997**, *43*, 2944.

36. He, C.-H. Infinite-Dilution Diffusion Coefficients in Supercritical and High-Temperature Liquid Solvents. *Fluid Phase Equilib.* **1998**, *147*, 309.

37. He, C.-H.; Yu, Y.-S. Estimation of Infinite-Dilution Diffusion Coefficients in Supercritical Fluids. *Ind. Eng. Chem. Res*. **1997**, *36*, 4430.

38. He, C.-H.; Yu, Y.-S. New Equation for Infinite-Dilution Diffusion Coefficients in Supercritical and High-Temperature Liquid Solvents. *Ind. Eng. Chem. Res*. **1998**, *37*, 3793.

39. Liu, H.; Silva, C. M.; Macedo, E. A. New Equations for Tracer Diffusion Coefficients of Solutes in Supercritical and Liquid Solvents Based on the Lennard-Jones Fluid Model. *Ind. Eng. Chem. Res*. **1997**, *36*, 246. Correction in *Ind. Eng. Chem. Res*. **1998**, *37*, 308.

40. Funazukuri, T.; Hachisu, S.; Wakao, N. Measurement of Binary Diffusion Coefficients of C16-C24 Unsaturated Fatty Acid Methyl Esters in Supercitical Carbon Dioxide. *Ind. Eng. Chem. Res*. **1991**, *30*, 1323.

41. Higashi, H.; Iwai, Y.; Takahashi, Y.; Uchida, H.; Arai, Y. Diffusion Coefficients of Naphthalene and Dimethylnaphthalene in Supercritical Carbon Dioxide. *Fluid Phase Equilib.* **1998**, *144*, 269.

42. Funazukuri, T.; Kong, C. Y.; Kagei, S. Effects of Molecular Weight and Degree of Unsaturation on Binary Diffusion Coefficients for Lipids in Supercritical Carbon Dioxide. *Fluid Phase Equilib.* **2004**, *219*, 67.

43. Funazukuri, T.; Kong, C. Y.; Kikuchi, T.; Kagei, S. Measurements of Binary Diffusion Coefficient and Partition Ratio at Infinite Dilution for Linoleic Acid and Arachidonic Acid in Supercritical Carbon Dioxide. *J. Chem. Eng. Data*. **2003**, *48*, 684.

44. Dariva, C.; Coelho, L. A. F.; Oliveira, J. V. Predicting Diffusivities in Dense Fluid Mixtures. *Brazilian J. Chem. Eng.* **1999**, *16*, 213.

45. Dariva, C.; Coelho, L. A. F.; Oliveira, J. V. A Kinetic Approach for Predicting Diffusivities in Dense Fluid Mixtures. *Fluid Phase Equilib.* **1999**, *158-160*, 1045.

46. Zhu, Y.; Lu, X.; Zhou, J.; Wang, Y.; Shi, J. Prediction of Diffusion Coefficients for Gas, Liquid and Supercritical Fluid: Application to Pure Real Fluids and Infinite Dilute Binary Solutions Based on the Simulation of Lennard-Jones Fluid. *Fluid Phase Equilib.* **2002**, *194-197*, 1141.

47. Rah, K.; Kwak, S.; Eu, B. C.; Lafleur, M. Relation of Tracer Diffusion Coefficient and Solvent Self-Diffusion Coefficient. *J. Phys. Chem. A.* **2002**, *106*, 11841.

48. Teja, A. S. Correlation and Prediction of Diffusion Coefficients by Use of a Generalized Corresponding States Principle. *Ind. Eng. Chem. Fundam.* **1985**, *24*, 39.

49. Medina, I.; Bueno, J. L. Solubilities of 2-Nitroanisole and 3-Phenyl-1-propanol in Supercritical Carbon Dioxide. *J. Chem. Eng. Data.* **2000**, *45*, 298.

50. González, L. M.; Bueno, J. L.; Medina, I. Determination of Binary Diffusion Coefficients of Anisole, 2,4-Dimethylphenol, and Nitrobenzene in Supercritical Carbon Dioxide. *Ind. Eng. Chem. Res*. **2001**, *40*, 3711.

51. Pitzer, K. S.; Schreiber, D. R. Improving Equation-of-State Accuracy in the Critical Region; Equations for Carbon Dioxide and Neopentane as Examples. *Fluid Phase Equilib.* **1988**, *41*, 1.

52. Stephan, K.; Lucas, K. *Viscosity of Dense Fluids*; Plenum.Press: New York, 1979.

53. Suárez, J. J.; Bueno, J. L.; Medina, I. Determination of Binary Diffusion Coefficients of Benzene and Derivatives in Supercritical Carbon Dioxide. *Chem. Eng. Sci*. **1993**, *48*, 2419.

54. Funazukuri, T.; Hachisu, S.; Wakao, N. Measurement of Diffusion Coefficients of C18 Unsaturated Fatty Acid Methyl Esters, Naphthalene and Benzene in Supercritical Carbon Dioxide by a Tracer Response Technique. *Anal. Chem.* **1989**, *61*, 118.

55. Liong, K. K.; Wells, P. A.; Foster, N. R. Diffusion of Fatty Acid Esters in Supercritical Carbon Dioxide. *Ind. Eng. Chem. Res.* **1992**, *31*, 390.

56. Sassiat, P. R.; Mourier, P.; Caude, M. H.; Rosset, R. H. Measurement of Diffusion Coefficients in Supercritical Carbon Dioxide and Correlation with the Equation of Wilke and Chang. *Anal. Chem.* **1987**, *59*, 1164.

57. Wells, T.; Foster, N. R.; Chaplin, R. P. Diffusion of Phenylacetic Acid and Vanillin in Supercritical Carbon Dioxide. *Ind. Eng. Chem. Res.* **1992**, *31*, 927.

58. Debenedetti, P. G.; Reid, R. C. Diffusion and Mass Transfer in Supercritical Fluids. *AIChE J.* **1986**, *32*, 2034.

59. Grushka, E.; Kikta, E. J. Jr.; Cullinan, H. T. Jr. Binary Liquid Diffusion Prediction in Infinitely Diluted Systems Using the Ultimate Volume Approach. *J. Phys. Chem*. **1976**, *80*, 757.

60. Filho, C. A.; Silva, C. M.; Quadri, M. B.; Macedo, E. A. Tracer Diffusion Coefficients of Citral and D-Limonene in Supercritical Carbon Dioxide. *Fluid Phase Equilib.* **2003**, *204*, 65.

61. Filho, C. A.; Silva, C. M.; Quadri, M. B.; Macedo, E. A. Infinite Dilution Diffusion Coefficients of Linalool and Benzene in Supercritical Carbon Dioxide. *J. Chem. Eng. Data.* **2002**, *47*, 1351.

62. Silva, C. M.; Filho, C. A.; Quadri, M. B.; Macedo, E. A. Binary Diffusion Coefficients of α-Pinene and β-Pinene in Supercritical Carbon Dioxide. *J. Supercrit. Fluids.* **2004**, *32*, 167.

63. Simons, J.; Ponter, A. B. Semiempirical Formulae for the Prediction of Diffusion in Liquid Systems. *Can. J. Chem. Eng*. **1975**, *53*, 541.

64. Alder, B. J.; Alley, W. E.; Dymond, J. H. Molecular Dynamics. XIV. Mass and Size Dependence of the Binary Diffusion Coefficient. *J. Chem. Phys*. **1974**, *61*, 1415.

65. Easteal, A. J.; Woolf, L. A. Tracer Diffusion in Hard-Sphere Liquids from Molecular Dynamics Simulations. *Chem. Phys. Lett*. **1990**, *167*, 329.

66. Chandler, D. Rough Hard-Sphere Theory of the Self-Diffusion Constant for Molecular Liquids. *J. Chem. Phys*. **1975**, *62*, 1358.

67. Dymond, J. H. Enskog Theory and the Transport Coefficients of Liquids. *J. Chem. Phys*. **1974**, *60*, 969.

68. Lide, R.D. *CRC Handbook of Chemistry and Physics* (80th ed); CRC Press: Boca Raton, **1999**.

69. Perry, R.H.; Green, D.W. *Chemical Engineer's Handbook* (Spanish edition); McGraw-Hill: Madrid, **2001**.

70. Gironi, G.; Lavecchia, R. Solubilities of Carbon Dioxide in Alkylaromatic Solvents at Low Pressure. *Fluid Phase Equilib.* **1992**, *78*, 335.

71. Yau, J. S.; Tsai, F. N. Correlation of Solubilities of Carbon Dioxide in Aromatic Compounds. *Fluid Phase Equilib*. **1992**, *73*, 1.

72. Groβ, T.; Buchhauser, J.; Lüdemann, H.-D. Self-Diffusion in Fluid Carbon Dioxide at High Pressures. *J. Chem. Phys.* **1998**, *109*, 4518.

FIGURES

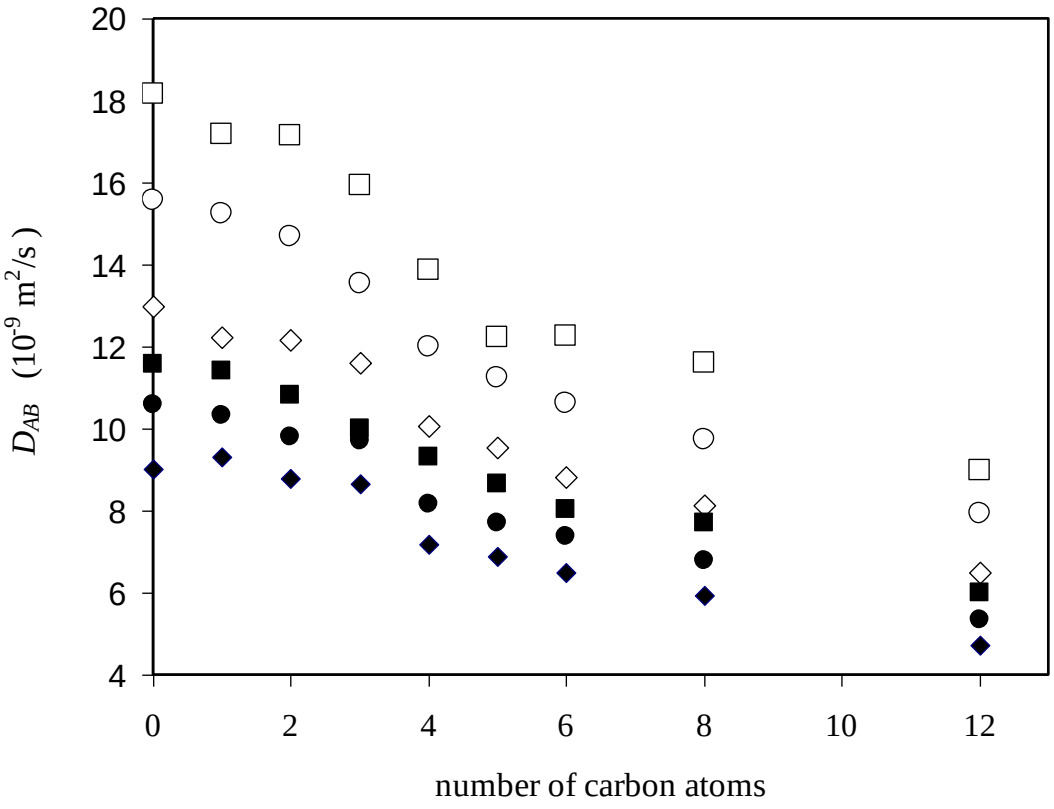

Figure 1. Binary diffusivities of alkylbenzenes as a function of carbon atoms in the radical chain: (□) at 15.0 MPa and 333 K, (○) at 15.0 MPa and 323 K, (◇) at 15.0 MPa and 313 K, (■) at 35.0 MPa and 333 K, (●) at 35.0 MPa and 323 K, (◆) at 35.0 MPa and 313 K.

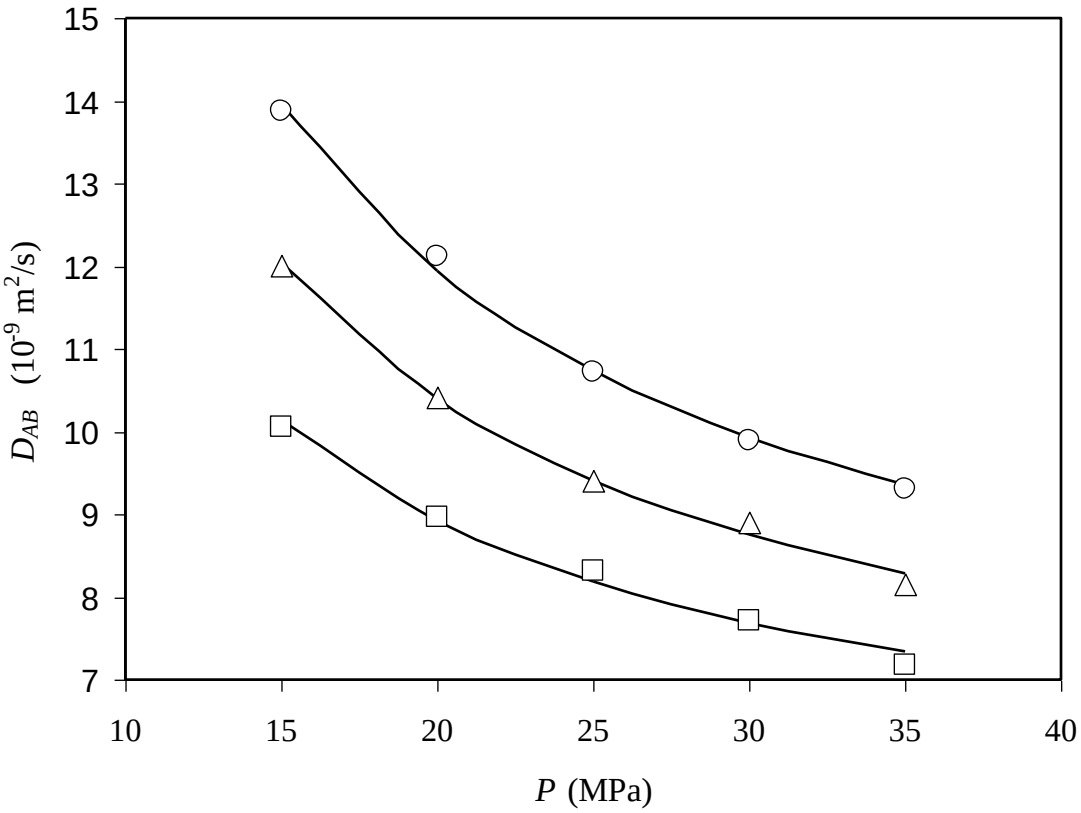

Figure 2. Binary diffusion coefficients of *n*-butylbenzene in carbon dioxide as a function of pressure: (□) at 313 K; (△) at 323 K; (○) at 333 K. The solid lines are the results of eq 3.

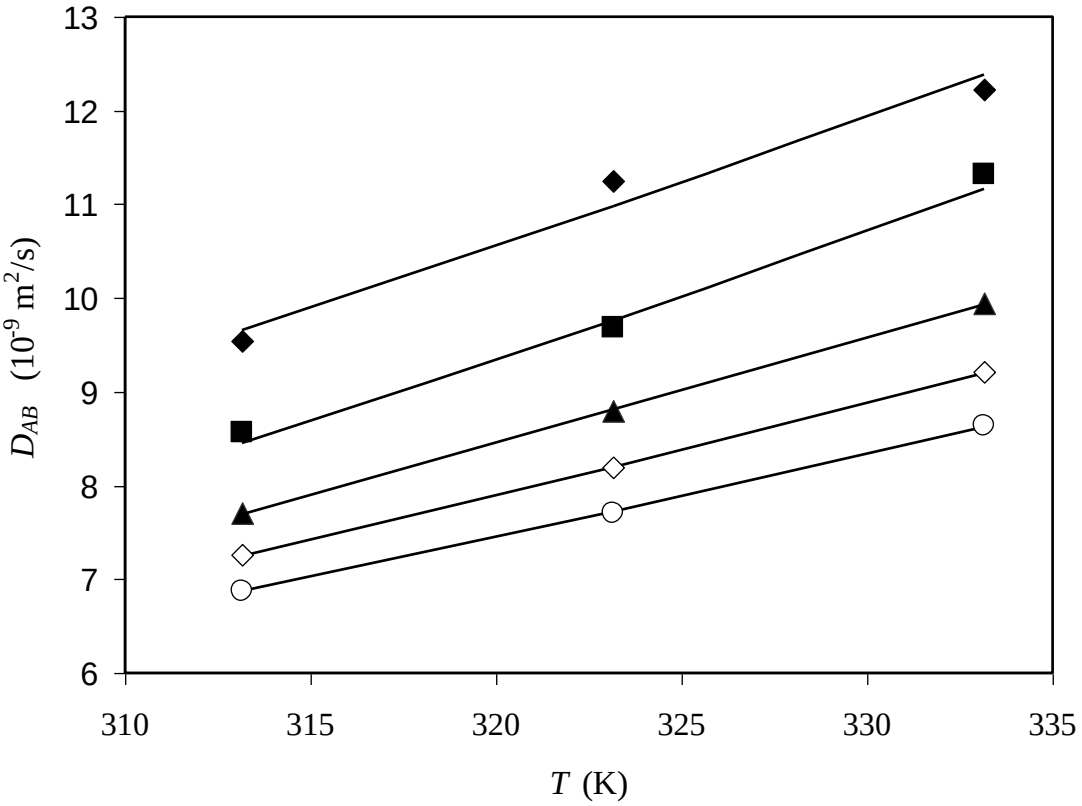

Figure 3. Binary diffusivities of *n*-pentylbenzene as a function of temperature: (◆) at 15.0 MPa; (■) at 20.0 MPa; (▲) at 25.0 MPa; (△) at 30.0 MPa; (○) at 35.0 MPa. The solid lines are the results of eq 4.

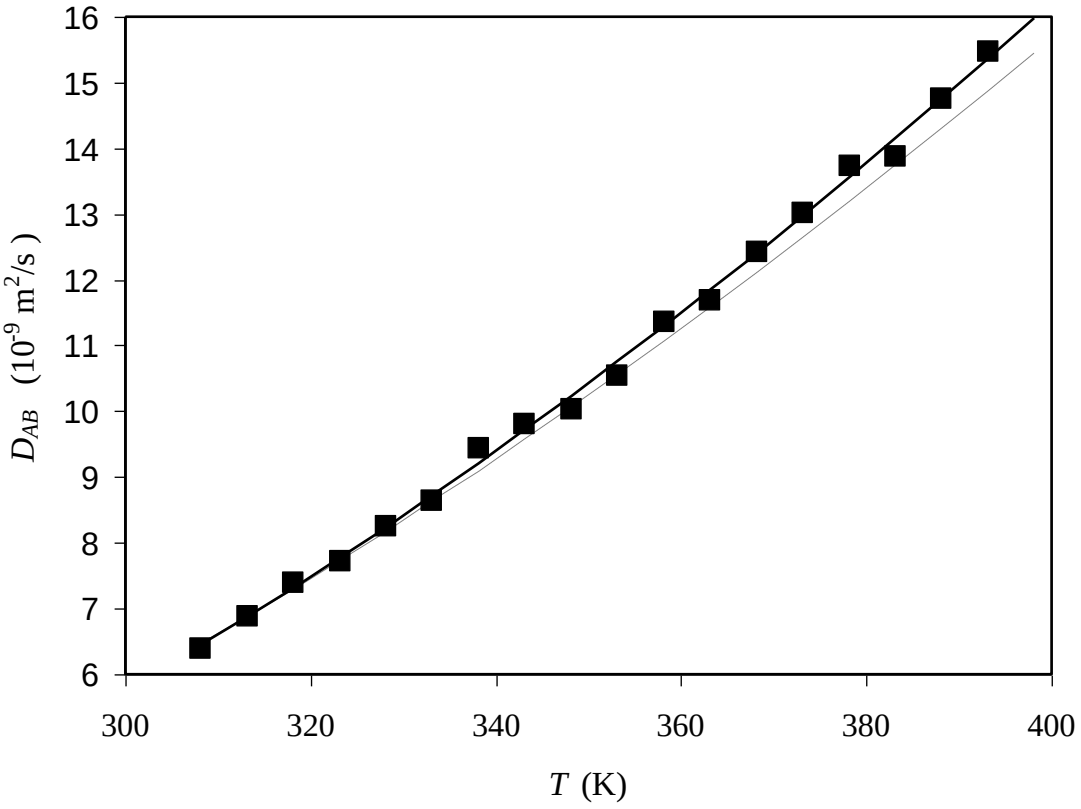

Figure 4. Binary diffusivities of *n*-pentylbenzene as a function of temperature at 35.0 MPa (■). The solid line is correlated with eq 4 and the parameters of Table 2 and the broken line is the extrapolation employing the same equation and the parameters of Table 1.

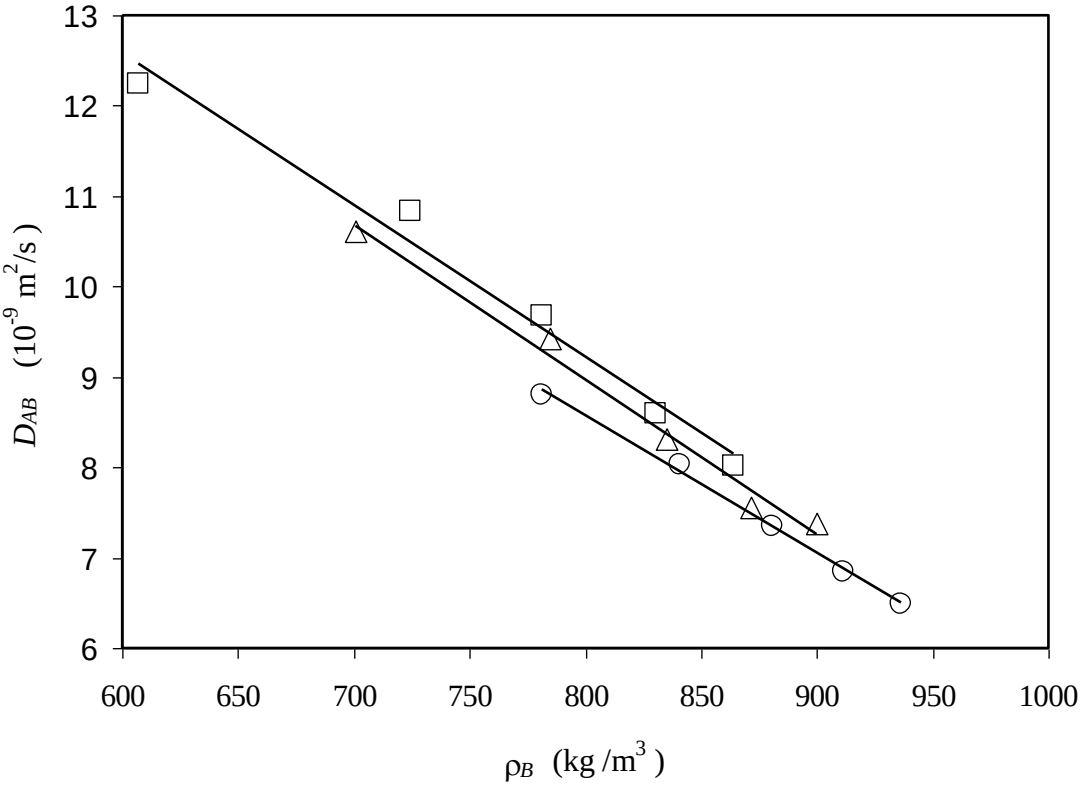

Figure 5. Density dependence on the binary diffusion coefficients of *n*-hexylbenzene in carbon dioxide: (□) at 333 K; (△) at 323 K; (○) at 313 K. The solid lines are the results of eq 7.

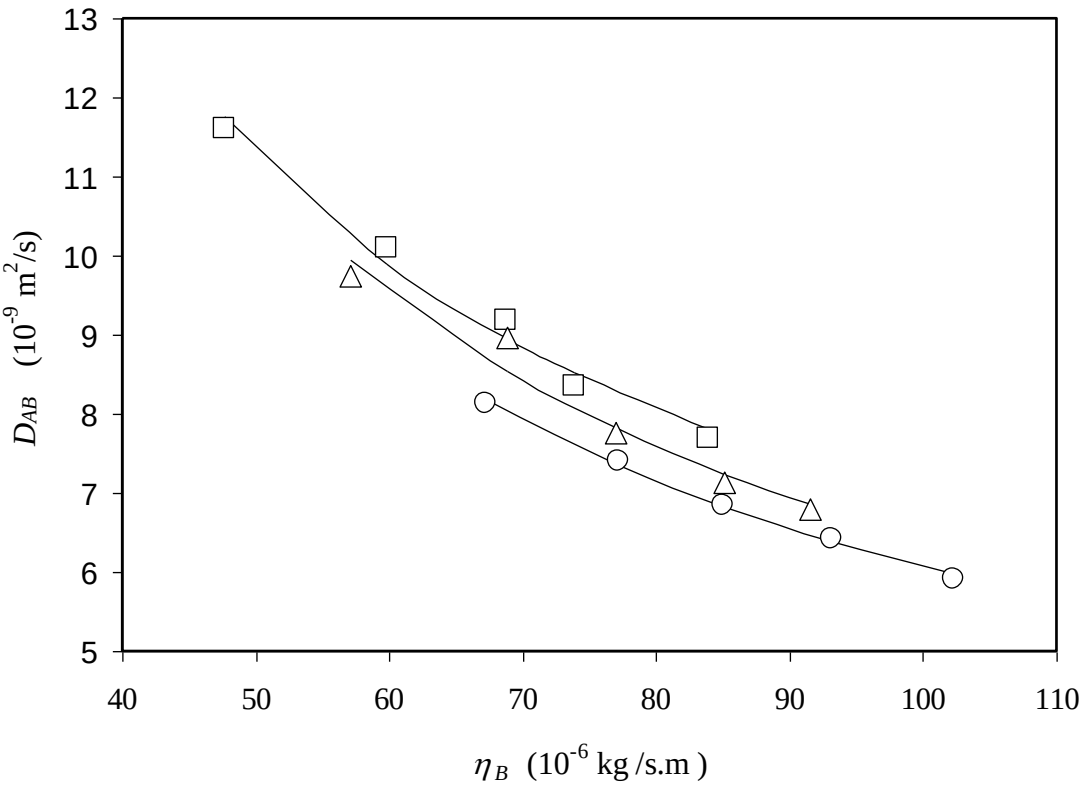

Figure 6. Viscosity dependence on the binary diffusion coefficients of 1-phenyloctane in carbon dioxide: (□) at 333 K; (△) at 323 K; (○) at 313 K. The solid lines are the results of eq 9.

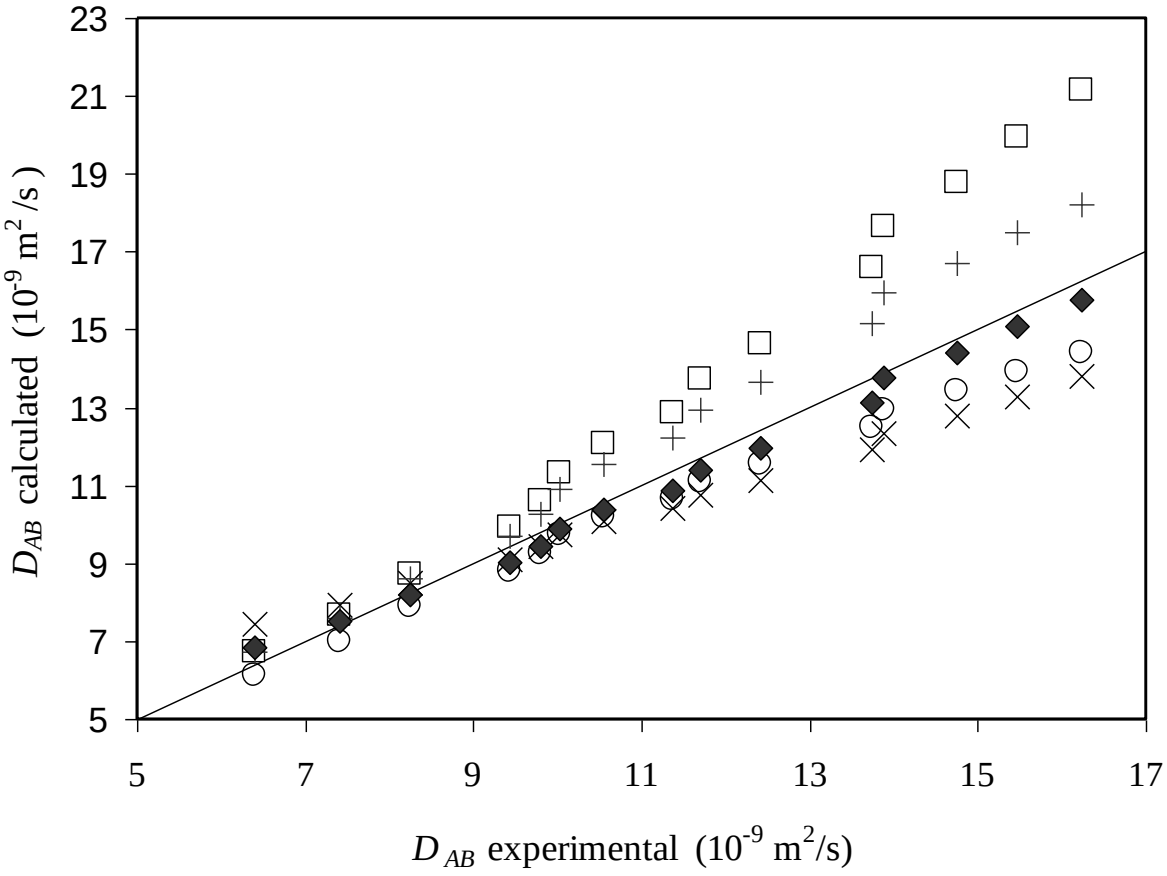

Figure 7. Comparison of the experimental and calculated diffusivities of *n*-pentylbenzene in carbon dioxide. (□) He of 1998; (+) Scheibel; (◆) He of 1997; (○) Funazukuri-Kong-Kagei; (×) Funazukuri-Hachisu-Wakao.

TABLES

Table 1. Experimental Results

T (K)	P (MPa)	ρ (kg/m^3)	η (10^{-6} kg/m s)	D_{AB} (10^{-9} m^2/s)				
				n-butylbenzene	*n*-pentylbenzene	1-phenylhexane	1-phenyloctane	1-phenyldodecane
313	15.0	781.0	67.2	10.05 ± 0.33	9.55 ± 0.15	8.81 ± 0.10	8.14 ± 0.07	6.49 ± 0.08
	20.0	840.8	77.2	8.97 ± 0.21	8.57 ± 0.09	8.03 ± 0.14	7.41 ± 0.16	5.77 ± 0.04
	25.0	880.7	85.0	8.32 ± 0.04	7.70 ± 0.07	7.35 ± 0.08	6.84 ± 0.06	5.42 ± 0.06
	30.0	911.2	93.1	7.71 ± 0.14	7.26 ± 0.05	6.85 ± 0.07	6.43 ± 0.05	5.01 ± 0.05
	35.0	936.1	102.3	7.18 ± 0.14	6.88 ± 0.08	6.49 ± 0.15	5.92 ± 0.02	4.73 ± 0.05
323	15.0	700.8	57.1	12.01 ± 0.39	11.25 ± 0.16	10.61 ± 0.22	9.75 ± 0.12	7.92 ± 0.13
	20.0	784.9	68.8	10.42 ± 0.24	9.68 ± 0.11	9.42 ± 0.23	8.96 ± 0.11	6.88 ± 0.03
	25.0	835.0	77.0	9.4 ± 0.21	8.80 ± 0.1	8.32 ± 0.09	7.77 ± 0.06	6.11 ± 0.05
	30.0	871.4	85.1	8.9 ± 0.18	8.19 ± 0.15	7.56 ± 0.05	7.14 ± 0.11	5.51 ± 0.24
	35.0	900.0	91.5	8.16 ± 0.07	7.71 ± 0.05	7.38 ± 0.06	6.80 ± 0.09	5.33 ± 0.08
333	15.0	607.1	47.6	13.87 ± 0.28	12.22 ± 0.50	12.25 ± 0.32	11.61 ± 0.52	9.00 ± 0.10
	20.0	724.6	59.8	12.13 ± 0.07	11.32 ± 0.13	10.83 ± 0.22	10.11 ± 0.13	8.11 ± 0.07
	25.0	781.2	68.7	10.73 ± 0.14	9.94 ± 0.04	9.68 ± 0.14	9.18 ± 0.28	7.14 ± 0.13
	30.0	830.5	73.8	9.90 ± 0.13	9.21 ± 0.32	8.59 ± 0.32	8.35 ± 0.10	6.22 ± 0.26
	35.0	864.0	83.9	9.31 ± 0.06	8.64 ± 0.05	8.02 ± 0.19	7.70 ± 0.06	5.99 ± 0.05

Table 2. Extra Diffusion Coefficient Data for *n*-Pentylbenzene at 35.0 MPa

T (K)	D_{AB} (10^{-9} m^2/s)	T (K)	D_{AB} (10^{-9} m^2/s)
308	6.39	363	11.69
318	7.40	368	12.42
328	8.25	373	13.02
338	9.43	378	13.73
343	9.80	383	13.87
348	10.02	388	14.75
353	10.54	393	15.47
358	11.36	398	16.24

Table 3. Properties of the Studied Substances

property	*n*-butylbenzene	*n*-pentylbenzene	1-phenylhexane	1-phenyloctane	1-phenyldodecane	carbon dioxide
T_c (K)	660.5	679.9	697.5	728.0	774.0	304.1
P_c (MPa)	28.9	26.0	23.8	20.4	15.8	7.38
T_b (K)	456.5	478.6	499.3	537.6	600.8	194.7
V_c (10^{-6} m^3/mol)	497.0	550.0	620.0	720.0	980.0	93.9
M (10^{-3} kg/mol)	134.00	148.25	162.27	190.33	246.44	44.01
ω	0.393	0.437	0.480	0.577	0.773	0.239
r_g (10^{-10} m)	4.849	4.792	5.071	5.584	6.517	0.992
ΔH_{vb} (kJ/mol)	39.246	41.212	43.095	46.861	54.392	23.08
area of van der Waals (10^{-20} m^2)	200.48	222.74	245.11	289.69	379.50	54.06
volume of van der Waals (10^{-30} m^3)	155.33	172.55	189.88	224.44	293.67	34.12
parachor ($g^{0.25}cm^3$/ mol $s^{0.5}$)	364.6	404.6	444.6	524.6	684.6	49.0
V_b (10^{-6} m^3/mol)	190.82	212.20	240.59	281.40	388.73	35.02

Table 4. AAD (%) for Predicting the Experimental Data of Table 1

equation	Ph-C_4	Ph-C_5	Ph-C_6	Ph-C_8	Ph-C_{12}
Stokes-Einstein type					
Scheibel	7.11	7.92	5.92	3.84	10.34
Wilke-Chang	6.25	6.57	7.65	9.77	5.90
Reddy-Doraiswamy	58.44	64.03	65.68	67.78	92.41
Lusis-Ratcliff	14.70	17.23	16.73	16.27	29.43
King-Hsue-Mao	14.42	17.66	18.68	18.30	32.89
Sitaraman-Ibrahim-Kuloor	6.80	4.80	3.68	3.20	11.70
Tyn-Calus	11.63	10.38	8.36	8.86	5.21
Umesi-Danner	8.24	3.92	3.27	3.46	16.56
Lai-Tan	16.63	21.45	23.72	26.56	48.09
Kooijman	31.60	34.55	35.67	34.22	52.24
Liu-Ruckenstein	5.27	8.24	9.16	7.75	18.51
Woerlee	29.03	29.06	31.21	33.87	31.69
rough-hard-sphere type					
Catchpole-King	7.59	6.59	5.83	6.11	7.09
Eaton-Akgerman	9.16	6.22	6.14	7.98	24.62
He of 1997	3.19	4.49	5.12	4.46	16.26
He of 1998	6.84	9.07	9.76	8.15	21.37
He-Yu of 1997	2.84	3.61	3.80	3.44	14.56
He-Yu of 1998	2.44	3.15	3.28	2.97	13.86
Liu-Silva-Macedo	14.46	13.82	13.85	15.74	5.73
Funazukuri-Hachisu-Wakao	6.94	7.19	6.97	5.67	14.06
Funazukuri-Kong-Kagei	2.94	3.36	3.07	3.19	10.65
Dariva-Coelho-Oliveira	14.91	14.60	14.57	15.83	9.58
Zhu-Lu-Zhou-Wang-Shi	9.37	11.18	11.20	12.67	17.52
Rah-Kwak-Eu-Lafleur	4.54	4.38	3.78	5.35	6.94
corresponding states principle with benzene and phenyldodecane					
eq.2 with $\theta = \omega$	9.27	11.48	12.63	5.54	---
eq.2 with $\theta = V_c^{2/3}$	5.22	7.37	6.86	2.99	---
corresponding states principle with benzene and phenyloctane					
eq.2 with $\theta = \omega$	7.00	8.46	8.81	----	10.85
eq.2 with $\theta = V_c^{2/3}$	3.96	5.74	4.76	----	5.54

Table 5. AAD (%) of the Best Equations of Table 4 for the 19 Points of *n*-Pentylbenzene at 35.0 MPa Ranging from 308 to 398 K

equation	AAD
Scheibel	8.81
Wilke-Chang	4.60
Sitaraman-Ibrahim-Kuloor	3.99
Umesi-Danner	3.08
He of 1997	2.89
He of 1998	15.97
He-Yu of 1997	2.93
He-Yu of 1998	3.79
Funazukuri-Hachisu-Wakao	8.98
Funazukuri-Kong-Kagei	6.37
Rah-Kwak-Eu-Lafleur	3.60

Supporting Information Available

Table 6. Fitting Parameters and Regression Coefficients of Equation 3

T (K)	fitting	*n*-butylbenzene	*n*-pentylbenzene	1-phenylhexane	1-phenyloctane	1-phenyldodecane
313	a_P (10^{-9} m^2/s)	5.23	4.90	4.84	4.49	3.51
	b_P (10^{-9} MPa m^2/s)	73.74	70.78	60.92	56.10	45.12
	R	0.9943	0.9973	0.9937	0.9886	0.9955
323	a_P (10^{-9} m^2/s)	5.47	5.09	4.77	4.55	3.28
	b_P (10^{-9} MPa m^2/s)	98.44	92.24	88.89	80.75	70.30
	R	0.9978	0.9999	0.9941	0.9849	0.9973
333	a_P (10^{-9} m^2/s)	5.90	6.06	4.97	4.97	3.68
	b_P (10^{-9} MPa m^2/s)	121.01	96.24	112.07	101.02	82.54
	R	0.9983	0.9829	0.9920	0.9962	0.9846

Table 7. Fitting Parameters and Regression Coefficients of Equation 4

P (MPa)	fitting	*n*-butylbenzene	*n*-pentylbenzene	1-phenylhexane	1-phenyloctane	1-phenyldodecane
15.0	a_T	7.6821	6.3878	7.6777	8.010	7.3372
	b_T (K^{-1})	-1681.9	-1290.0	-1721.3	-1852.0	-1708.9
	R	0.9990	0.9856	0.9984	0.9999	0.9942
20.0	a_T	7.2174	6.7638	7.0698	7.1002	7.4238
	b_T (K^{-1})	-1573.7	-1449.5	-1561.1	-1624.0	-1775.9
	R	0.9997	0.9960	0.9998	0.9939	1.0000
25.0	a_T	6.3501	6.2961	6.5697	6.8081	6.2665
	b_T (K^{-1})	-1326.0	-1332.3	-1434.5	-1532.3	-1435.4
	R	0.9991	0.9999	0.9971	0.9955	0.9957
30.0	a_T	6.2171	5.9441	5.6828	6.1935	5.2042
	b_T (K^{-1})	-1305.8	-1240.9	-1178.8	-1359.8	-1126.8
	R	0.9977	0.9999	0.9958	0.9913	0.9962
35.0	a_T	6.2949	5.7207	5.4093	6.1595	5.4864
	b_T (K^{-1})	-1354.6	-1187.9	-1106.3	-1371.7	-1231.7
	R	0.9996	0.9998	0.9945	0.9999	0.9999

Table 8. Fitting Parameters and Regression Coefficients of Equations 4, 5 and 6 for *n*-Pentylbenzene

parameter	numerical value	*R*
a_T	5.88	0.9991
b_T (K^{-1})	-1237.6	
$a_T^{(I)}$	-18.57	0.9988
$b_T^{(I)}$	3.57	
$a_T^{(II)}$ (10^9 m^2/s)	-26.31	0.9967
$b_T^{(II)}$ (10^9 m^2/K s)	0.1055	

Table 9. Fitting Parameters and Regression Coefficients of Equation 7

T (K)	fitting	*n*-butylbenzene	*n*-pentylbenzene	1-phenylhexane	1-phenyloctane	1-phenyldodecane
313	a_ρ (10^{-9} m^2/s)	24.351	23.252	20.723	19.166	15.253
	b_ρ (10^{-12} $m^5/s.kg$)	-18.283	-17.541	-15.193	-14.044	-11.230
	R	0.9991	0.9981	0.9986	0.9964	0.9986
323	a_ρ (10^{-9} m^2/s)	25.315	23.672	22.682	20.853	17.423
	b_ρ (10^{-12} $m^5/s.kg$)	-18.985	-17.773	-17.136	-15.602	-13.530
	R	0.9986	0.9997	0.9937	0.9862	0.9968
333	a_ρ (10^{-9} m^2/s)	24.966	21.198	22.633	20.917	16.691
	b_ρ (10^{-12} $m^5/s.kg$)	-18.094	-14.356	-16.756	-15.137	-12.344
	R	0.9986	0.9785	0.9909	0.9964	0.9821

Table 10. Fitting Parameters and Regression Coefficients of Equation 8

fitting	*n*-butylbenzene	*n*-pentylbenzene	1-phenylhexane	1-phenyloctane	1-phenyldodecane
$a_{\rho T}$ (10^{-9} m^2/K s)	0.0773	0.0682	0.0686	0.0648	0.0514
$b_{\rho T}$ (10^{-15} m^5/K s kg)	-57.625	-49.034	-51.181	-48.635	-38.845
R	0.9971	0.9874	0.9945	0.9917	0.9912

Table 11. Fitting Parameters and Regression Coefficients of Equation 9

T (K)	fitting	*n*-butylbenzene	*n*-pentylbenzene	1-phenylhexane	1-phenyloctane	1-phenyldodecane
313	a_η (10^{-9} m^2/s)	1.6769	1.5194	1.8893	1.7424	1.328
	b_η (10^{-12} kg m/s)	563.01	538.35	467.16	432.97	345.67
	R	0.9999	0.9955	0.9979	0.9983	0.9990
323	a_η (10^{-9} m^2/s)	2.0263	1.8586	1.6606	1.7343	0.8209
	b_η (10^{-12} kg m/s)	572.38	536.62	516.68	468.86	408.27
	R	0.9973	0.9998	0.9925	0.9817	0.9964
333	a_η (10^{-9} m^2/s)	3.1213	3.8863	2.4412	2.6493	1.838
	b_η (10^{-12} kg m/s)	518.72	410.24	477.96	433.45	350.72
	R	0.9926	0.9717	0.9822	0.9916	0.9697

Table 12. Fitting Parameters and Regression Coefficients of Equation 10

fitting	*n*-butylbenzene	*n*-pentylbenzene	1-phenylhexane	1-phenyloctane	1-phenyldodecane
$a_{\eta T}$ (10^{-9} m^2/K s)	0.0068	0.0083	0.0060	0.0053	0.0039
$b_{\eta T}$ (10^{-15} kg m /K s)	1.7122	1.4531	1.5191	1.4438	1.1513
R	0.9932	0.9809	0.9894	0.9869	0.9848